

Journal of Materials Chemistry A

Accepted Manuscript



This is an *Accepted Manuscript*, which has been through the Royal Society of Chemistry peer review process and has been accepted for publication.

Accepted Manuscripts are published online shortly after acceptance, before technical editing, formatting and proof reading. Using this free service, authors can make their results available to the community, in citable form, before we publish the edited article. We will replace this *Accepted Manuscript* with the edited and formatted *Advance Article* as soon as it is available.

You can find more information about *Accepted Manuscripts* in the [Information for Authors](#).

Please note that technical editing may introduce minor changes to the text and/or graphics, which may alter content. The journal's standard [Terms & Conditions](#) and the [Ethical guidelines](#) still apply. In no event shall the Royal Society of Chemistry be held responsible for any errors or omissions in this *Accepted Manuscript* or any consequences arising from the use of any information it contains.

ARTICLE

Edge-Iodine/Sulfonic Acid-Functionalized Graphene Nanoplatelets as an Efficient Electrocatalyst for Oxygen Reduction Reaction

Cite this: DOI: 10.1039/x0xx00000x

Jong Yeol Baek,^a In-Yup Jeon^a and Jong-Beom Baek^{*a}Received 00th January 2012,
Accepted 00th January 2012

DOI: 10.1039/x0xx00000x

www.rsc.org/

We report the synthesis of edge-iodine/sulfonic acid-functionalized, graphene nanoplatelets (ISGnP) *via* two-step sequential ball-milling of graphite, and their use as electrocatalyst for oxygen reduction reaction (ORR) in fuel cells. The graphite is ball-milled in the presence of iodine to produce edge-iodine functionalized GnP (IGnP) in the first step and the IGnP is subsequently ball-milled with sulfur trioxide to yield ISGnP. The resultant ISGnP is highly dispersible in various polar solvents, allowing the fabrication of electrodes for ORR using solution processing. The capacitance and cycle stability of ISGnP in an alkaline medium is superior to commercial Pt/C and its kinetic electron transfer number (*n*) is comparable to the Pt/C.

Introduction

The oxygen reduction reaction (ORR) in fuel cells is currently most often enhanced using platinum (Pt)-based electrocatalysts. However, this approach suffers from their high cost, low fuel selectivity and poor durability.¹ Therefore, active research has recently been aimed at replacing the vulnerable Pt-based electrocatalysts in fuel cells.² Metal-free, heteroatom-doped, carbon-based nanomaterials have provided candidates of great potential,¹ because the heteroatom in a graphitic framework can induce electron modulation of the carbon network that enhances electrocatalytic activities.³ There are numerous approaches to prepare the heteroatom-doped carbon nanomaterials. Several representative approaches (*e.g.*, chemical vapor deposition (CVD)⁴ and chemical derivatization of graphite oxide (GO)^{5,6}) have been investigated for the purpose of introducing heteroatoms (*e.g.*, boron,⁷ pnictogens,⁸ chalcogens⁹ and halogens^{10,11}) into graphitic frameworks. Although the CVD method can produce high-quality doped graphene nanoplatelets (GnPs),⁴ it requires meticulous technical elaborations and thus is not cost-effective for scalable production of practical uses. The solution-exfoliation of graphite into GO allows the mass production of GnPs. However, the method involves strong, hazardous oxidizing reagents (*e.g.*, HNO₃, KMnO₄, H₂SO₄) and a tedious multi-step process.¹² After the exfoliation of graphite into GO, a reduction of GO into reduced graphene oxide (rGO) requires even more hazardous reducing reagents (*e.g.*, hydrazine, NaBH₄).^{5,13,14} These treatments, which use highly destructive reagents, lead to severe physical and chemical

damage to the graphitic frameworks; thus diminishing unique properties, such as electrical characteristics and structural integrity, arising from the extreme crystallinity of the graphitic structure.¹⁵ Recently, we developed an alternative method to overcome the limitations of the CVD and GO approaches. The newly-developed mechanochemical, ball-milling process allows the introduction of various functional groups at the cracked edges of GnPs.¹⁶ The mechanism involves mechanochemical cracking of graphitic C-C bonds to generate reactive carbon species; which induces edge-selective functionalization at the cracked edges and subsequent delamination of graphitic layers into a few layer GnPs. As a result, the mechanochemical process is a simple, low-cost, eco-friendly, scalable approach to produce GnPs with a variety of desirable functions, and with minimal distortion of the basal plane.¹⁶⁻¹⁹

On the basis of an optimized condition for this mechanochemical process, we hybridized two systems to promote the best electrocatalytic activity for oxygen reduction reaction (ORR) in fuel-cells. Addition of an ionic iodine group (C-I⁺-C) to the edge-iodine/sulfonic acid-functionalized GnPs (ISGnP) thermodynamically contributed to charge polarization that enhanced ORR performance.¹¹ Further addition of a sulfonic acid group to the ISGnP kinetically contributed to efficient oxygen diffusion which improved ORR performance.¹⁷ As a result, the ISGnP was expected to exhibit synergistically enhanced ORR performance. Thus, ISGnP was prepared by two-step, sequential ball-milling of graphite in the presence of iodine in the first step, and with sulfur trioxide in

the following step. The resultant ISGnP, disperses well in many polar solvents; leading to feasible solution processes for many practical applications. In this work, metal-free cathodes were fabricated for fuel-cell applications. The ISGnP displayed high electrocatalytic activity in an alkaline electrolyte (0.1M aq. KOH solution), and was superior to Pt-based electrocatalyst in terms of current density and cycle stability for practical use.

Experimental

Instrumentation

Fourier transform infrared (FT-IR) spectra were recorded on Perkin-Elmer Spectrum 100 using KBr pellets. TGA were conducted on a TA Q200 (TA Instrument) under air and nitrogen with a ramping rate of 10 °C/min. The surface area was measured by nitrogen adsorption-desorption isotherms using the Brunauer-Emmett-Teller (BET) method on a Micromeritics ASAP 2504N. The field-emission scanning electron microscopy (FE-SEM) was performed on an FEI Nanonova 230. X-ray photoelectron spectra (XPS) were recorded on a Thermo Fisher K-alpha XPS spectrometer. Elemental analysis (EA) was conducted with the Thermo Scientific Flash 2000. X-ray diffraction (XRD) patterns were recorded with a Rigaku D/MAZX 2500 V/PC with Cu-K α radiation (35 kV, 20 mA, $\lambda = 1.5418 \text{ \AA}$). Raman spectra were taken with a He-Ne laser (532 nm) as the excitation source using confocal Raman microscopy (Alpha 300S, WITec, Germany). Contact angle measurements were conducted on a Kratos DSA 100 contact-angle analyzer. Sample solutions were coated on a silicon (Si) wafer.

Procedure for the preparation of ISGnP by stepwise ball-milling of graphite in the presence of iodine and sulphur trioxide

In a typical experiment, the ball-milling of graphite was carried out in a planetary ball-milling machine (Pulverisette 6, Fritsch) in the presence of iodine and sulfur trioxide at 500 rpm for 24 hours for each step.

For the first step, pristine graphite (5.0 g, Alfa Aesar, natural graphite, 100 mesh, < 150 μm , 99.9995% metals basis, lot # 14735) and iodine (10.0 g, Aldrich Chemical Inc., $\geq 99.8\%$) were placed into a stainless steel capsule containing stainless steel balls (500 g, diameter: 5 mm). After five cycles of argon charge and discharge through the gas inlet, the capsule was fixed in the ball-mill machine and agitated at 500 rpm for 24 h. The intermediate, edge-iodine-functionalized graphene nanoplatelets (IGnP) were completely worked-up by Soxhlet extracted with 1 M aq. HCl solution to completely acidify the residual active species and to remove metallic impurities (e.g., iron oxide), if any. Further Soxhlet extraction with methanol was conducted to get rid of residual iodine. The resultant IGnP was freeze-dried at $-120 \text{ }^\circ\text{C}$ under reduced pressure (0.05 mmHg) for 48 h to yield 6.2 g (at least 1.2 g of iodine uptake) of dark black powder.

For the second step, the IGnPs (5.0 g) and stainless steel balls (500 g, diameter: 5 mm) were placed in the capsule. After five

cycles of argon charge and discharge, sulfur trioxide (9.0 g, Aldrich Chemical Inc.) was injected through the gas inlet. The capsule was agitated at 500 rpm for 24 h and worked-up following the procedure used for IGnPs to produce ISGnP (4.57g) of dark black powder.

Results and Discussion

Structural information

Iodine/sulfonic acid co-doped graphene nanoplatelets (ISGnP) were prepared by sequential ball-milling of graphite in the presence of iodine and sulfur trioxide (Fig. 1a). In the first ball-milling step, edge-selective iodine-doped GnP (IGnP) was prepared by ball-milling of graphite (100 mesh, < 150 μm) in the presence of iodine. In the second ball-milling step, the intermediate IGnP was further cracked in the ball-mill crusher in the presence of sulfur trioxide to yield ISGnP (see Experimental section). As described in Fig. 1a, the mechanism of edge-selective functionalization *via* mechanochemical ball-milling can be explained. The reactive carbon species (mostly radicals or ions) are generated by cleavage of graphitic C-C bonds at the broken edges.^{6,11,16} The reactive carbon species react with iodine to produce IGnP, and subsequently with sulfur trioxide to produce ISGnP during sequential ball-milling. After ball-milling, the remnant active carbon species were terminated by exposure to air moisture, and subsequent Soxhlet extraction with aqueous medium introducing additional hydroxyl (-OH) and carboxylic acid (-COOH) at the edges of the ISGnP.^{6,11,16}

Scanning electron microscope (SEM) images show obvious changes in morphology before (pristine graphite, Fig. 1b) and after (ISGnP, Fig. 1c) ball-milling. The pristine graphite displays a large, flake-shape with grain size in the range of a few tens of micrometers (Fig. 1b). On the other hand, the ISGnP shows aggregated morphology with a wrinkled surface probably due to the polar nature of sulfonic acid at the edges, and due to reduced grain size in the range of 0.1-1 μm as a result of mechanochemical cracking (Fig. 1c).

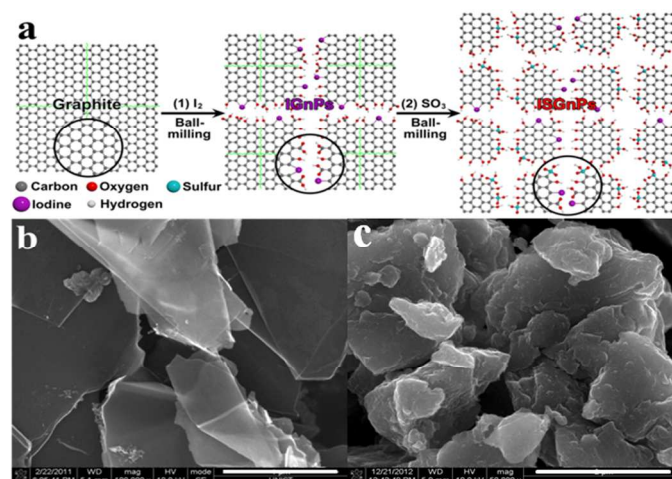


Fig. 1. (a) Schematic representation of stepwise ball-milling of graphite in the presence of: (1) iodine and (2) sulfur trioxide to produce ISGnPs. SEM images: (b) pristine graphite; (c) ISGnP. Scale bars are 1 μm .

To illustrate the bonding nature of ISGnP, the FT-IR analysis was presented in Fig. 2a. A broad, O-H stretching peak is observed at around $3,425\text{ cm}^{-1}$, due to bound moisture and sulfonic acid ($-\text{SO}_3\text{H}$). The peaks at $2,920$ and $2,850\text{ cm}^{-1}$ are due to sp^3 and sp^2 C-H stretching, respectively. The C=O and C-O stretching peaks from carboxyl acid ($\text{O}=\text{C}-\text{OH}$) are located at $1,715$ and $1,230\text{ cm}^{-1}$, respectively. The C=C stretching peak corresponding to the extended conjugated C=C bond of graphitic framework is at $1,585\text{ cm}^{-1}$. The S=O and S-O stretching peaks for $-\text{SO}_3\text{H}$ appeared at $1,400$ and 825 cm^{-1} , respectively. The relatively weak bands of $-\text{SO}_3\text{H}$ can be interpreted, because of the perturbation of the strong inter- and intra-molecular hydrogen bonding.¹⁷ Finally, the C-I stretching peak was detected at around 600 cm^{-1} . The FT-IR results indicate that iodine and sulfonic acid have been introduced in the ISGnP *via* mechanochemical ball-milling.

The elemental composition of ISGnP was further characterized using elemental analysis (EA), energy dispersive X-ray (EDX) and X-ray photoelectron spectroscopy (XPS). As summarized in Table S1, elemental composition is presented in terms of weight percent (wt.%) for EA, and atomic percent (at.%) for EDX (Fig. S1) and XPS. The carbon content of the pristine graphite was in the range of 98.35 - 99.64%, while that of ISGnP was significantly less (74.52 - 83.55%), implying that heteroatoms had been introduced at the edges of ISGnP. We could identify the presence of iodine and sulfur, together with oxygen (Table S1). The XPS survey of ISGnP also displays the presence of iodine and sulfur elements (Fig. 2b). The high-resolution XPS spectra show that the C 1s core-level of ISGnP is divided into five curves at 284.3 (C=C), 285.1 (C-O), 286.5 (C-S), 288.2 (C=O) and 290.1 (C=C plasmon) (Fig. S2a).²⁰ The O 1s core level of the ISGnP can be deconvoluted into two curves at 531.4 (O=C=O, S=O), and 533 (C-O-H) (Fig. S2b). The S 2p core level of the ISGnP is divided into three peaks at 163.3 (C-S), 164.5 (C-S) and 167.6 (S=O) (Fig. S2c). The I 3d core level of ISGnP gives four peaks at 618.8 (C-I semi-ionic, $\text{Id}_{5/2}$), 620.8 (C-I covalent, $\text{Id}_{5/2}$), 630 (C-I semi-ionic, $\text{Id}_{3/2}$) and 631.5 (C-I covalent, $\text{Id}_{3/2}$) (Fig. S2d).²¹

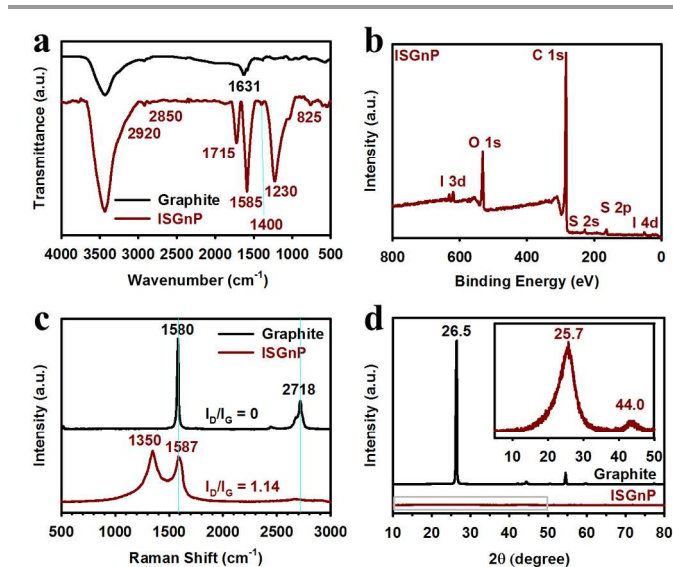


Fig. 2. (a) FT-IR spectra; (b) XPS survey spectrum; (c) Raman spectra; (d) XRD patterns. The top right inset within (d) is magnification of the gray rectangle (lower left inset).

Thermogravimetric analysis (TGA) was conducted to quantitatively estimate the degree of functionalization. Pristine graphite was stable up to $750\text{ }^\circ\text{C}$ at one atmosphere. Weight loss of ISGnP occurred around $100\text{ }^\circ\text{C}$, and major thermo-oxidative weight loss occurred at around $480\text{ }^\circ\text{C}$ (Fig. S3a). The early weight loss could be attributed to bound moisture, and the catastrophic weight loss at around $480\text{ }^\circ\text{C}$ could be related to heavy functionalization and grain-size reduction of ISGnP. In nitrogen, the pristine graphite experienced negligible weight loss ($\sim 0.9\text{ wt.}\%$) up to $1000\text{ }^\circ\text{C}$ (Fig. S3b). On the basis of char yield at $1000\text{ }^\circ\text{C}$, the difference between structurally robust, pristine graphite and ISGnP could provide a rough estimation of the amount of functional groups ($28.3\text{ wt.}\%$, Table S1). The weight loss for ISGnP was mainly attributed to the thermal decomposition of the edge functional groups *via* dehydration, decarboxylation, desulfonation and deiodination into moisture, carbon dioxide, sulfur trioxide and iodine in that order.¹⁶ The weight loss ($28.3\text{ wt.}\%$) determined by the TGA analysis agreed quite well with the EA result ($25.5\text{ wt.}\%$) (Table S1).

The Raman spectra are shown in Fig. 2c. Due to the undisturbed large grain size of the pristine graphite, a D-band related to edge distortions and other topological defects does not appear around $1,350\text{ cm}^{-1}$ (Fig. 2c). In contrast, ISGnP shows a strong D-band at $1,350\text{ cm}^{-1}$ with an I_D/I_G ratio of 1.14, which indicates that mechanochemical cracking by ball-milling has induced significant grain-size reduction and edge-functionalization of ISGnP as described in Fig. 1.¹⁷

X-ray diffraction (XRD) was used to estimate the degree of ISGnP delamination (Fig. 2d). The XRD pattern of the pristine graphite showed a typical strong [002] peak at 26.5° associated with an interlayer d -spacing of 0.34 nm of hexagonal graphite.²² In contrast, ISGnP shows a weak (less than 0.01% of pristine graphite), broad peak around 25.7° (d -spacing of 0.35 nm , inset in Fig. 2d), signifying edge-delamination of graphitic

layers after functionalization even in the solid state.¹⁷ Therefore, the ball-milling induces not only mechanochemical cracking of large graphitic layers into small fragments but also functionalization at the cracked edges, resulting in significant delamination of graphitic layers into GnP.¹⁷ Further exfoliation of ISGnP upon dispersion in solvents could also be expected (*vide infra*).

Fig. S4a demonstrates that ISGnP disperses well in various solvents, not only in aqueous media (small white oval) such as water and aqueous ammonium hydroxide, but also in polar protic and aprotic solvents (large white oval) such as alcohols, acetone, *N,N*-dimethylformamide (DMF), *N,N*-dimethylacetamide (DMAc), and *N*-methyl-2-pyrrolidone (NMP). Due to the presence of polar-acidic edge-functional groups (*e.g.*, including OH, COOH and SO₃H) at its edges, ISGnP is poorly dispersible in aqueous acidic media (*e.g.*, aqueous hydrochloric acid), nonpolar solvents (*e.g.*, toluene, dichloromethane and hexane), and ether solvents. The dispersion stability of ISGnP in NMP was evaluated using Zeta potential measurement. The values were -43.4, -45.4 and -43.6 mV at the concentrations of 0.4, 0.5 and 0.6 mg/mL, respectively (Table S2). The result indicated that the negatively charged sulfonate groups (-SO₃⁻) of the sulfonic acids contributed to good dispersion stability of ISGnP in basic NMP medium. Hence, the high dispersion stability of ISGnP allows good solution processability (Table S3), leading to uses in many practical applications. Fig. S4b shows a contact-angle snapshot, which describes the nature of the polar surfaces of ISGnP. Generally, if the water contact angle is greater than 90°, the solid surface is considered hydrophobic.²³ ISGnP has a contact angle of 51°, so it is considered hydrophilic like the surface of silicon oxide (SiO₂) (Fig. S4c) and it displays much lower contact angle than the hydrophobic surface (118°) of pristine graphite (Fig. S4d). Although the ISGnP was expected to possess a more hydrophilic nature than SiO₂ due to the polar functional groups (*e.g.*, OH, COOH, SO₃H) at its edges, it displayed a higher contact angle than SiO₂. This is because of the presence of much less hydrophilic iodine, which repels water molecules and thus minimizes its contact area with the surface of ISGnP. As a result, the interaction between the ISGnP and water was somewhat diminished, and its contact angle was less than that for silicon wafer.

Electrochemical Study for Electrocatalyst in Fuel Cells

Given the structural information, ISGnP was finally evaluated for potential use as an electrocatalyst in fuel cells. The heteroatoms in ISGnP (*e.g.*, iodine, sulfur and oxygen) could polarize ISGnP to enhance electrocatalytic activity.²⁴ Polar heteroatom-doping enables stable adsorption onto the surface of functionalized graphitic electrodes (thermodynamic contribution)¹¹ and rapid oxygen diffusion to the electrode (kinetic contribution).¹⁷ On the basis of previous study, edge-iodinated GnPs (IGnP) displayed high charge polarization, due to the formation of -I⁺- bond¹¹ and edge-sulfonated GnPs (SGnP) had high polarity contributed to -SO₃H (existed as -SO₃⁻ in alkaline electrolyte).¹⁷ The polar nature of ISGnP is

expected to help the efficient oxygen absorption onto edge active sites and thus to improve electrochemical performance.¹⁷ For the purpose of comparison, the pristine graphite (much bigger grain size than ISGnP), edge-hydrogen functionalized GnP (HGnP,¹⁷ similar grain size with ISGnP) and platinum on activated carbon (Pt/C, Vulcan XC-72R, commercial ORR electrocatalyst) were tested under the same conditions. The HGnP was prepared *via* ball-milling of graphite under H₂ gas.¹⁷ Typical cyclic voltammograms (CV) in alkaline electrolyte under nitrogen-saturated condition showed that ISGnP has much better electrochemical capacitance than pristine graphite and HGnP (Fig. 3a and Table S4). The capacitance of ISGnP (108.8 F/g) is even better than Pt/C (90.1 F/g). When oxygen saturated, ISGnP displays superb electrocatalytic activity in relation to the reference samples (Fig. 3b and Table S4). In addition, ISGnP showed significantly improved onset potential of ORR compared to pristine graphite and HGnP (sky blue arrow, Fig. 3b). This expected result implies that ISGnP contributes to efficient oxygen diffusion and adsorption. For example, the BET surface area of ISGnP (6.03 m²/g) is much less than that of HGnP (437 m²/g), but the specific capacitance of ISGnP is much greater (Table S5). This can be explained by the high polarity of the ionic iodine (C-I⁺-C) and sulfonate (-SO₃⁻) of ISGnP in the alkaline medium, which contribute to increased double-layer capacitance by enhancing charge polarization (thermodynamics)¹¹ and oxygen diffusion (kinetics).¹⁷ Together, these overcome the disadvantage of its small surface area. More importantly, the ISGnP showed better cycle stability than Pt/C under prolonged use (10,000 cycles, Fig. S5). ISGnP exhibited capacitance retentions of 77.1 and 66.4% under nitrogen and oxygen-saturated conditions respectively, while Pt/C retained only 57.7 and 53.4% (Table S6). The ORR kinetics of ISGnP was studied using a rotating disk electrode (RDE, Fig. 4) and analyzed using the Koutecky–Levich equation (Supporting Information). Fig. 5 shows that the current density increases as the rotation rate increases, because the flux of electroactive species to the surface of the electrode increases by convection force. As summarized in Table S7, the electron transfer number (*n*) of the ISGnP was increased from 2.8 to 4.0 as the applied potential increased from -0.4 to -0.6 V, which is a typical potential range of fuel-cell operation.²⁵ This result indicates that use of ISGnP as an electrocatalyst could efficiently facilitate ORR. Hence, introduction of iodine (I) and sulfonic acid (-SO₃H) at the edges of graphitic layers was found to produce good ORR performance with higher capacitance and better cycle stability than commercial Pt/C electrocatalyst. These results provide insights into the design of carbon-based materials as alternatives to expensive Pt-based electrocatalysts for cathodic ORR in fuel cells.

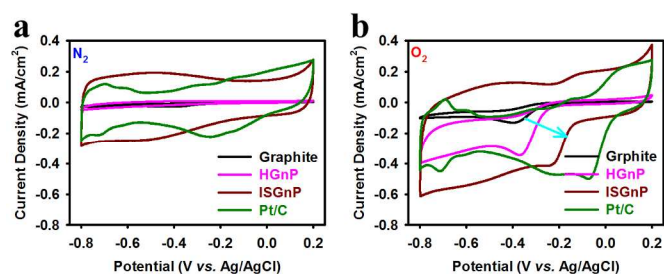


Fig. 3. Cyclic voltammograms (CV) of samples on glassy carbon (GC) electrodes in 0.1 M aq. KOH solution; with scan rate of 10 mV/s: (a) Nitrogen-saturated; (b) Oxygen-saturated.

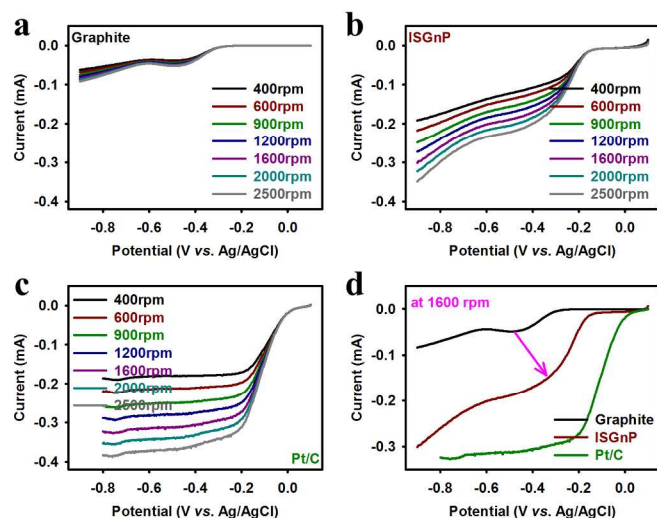


Fig. 4. RDE voltammograms in oxygen-saturated 0.1 M aq. KOH solution with a scan rate of 10 mV/s at different rotating rates of 400, 600, 900, 1200, 1600, 2000 and 2500 rpm: (a) the pristine graphite; (b) ISGnP; (c) Pt/C; (d) comparison of RDE voltammograms of sample electrodes at a rotation rate of 1600 rpm.

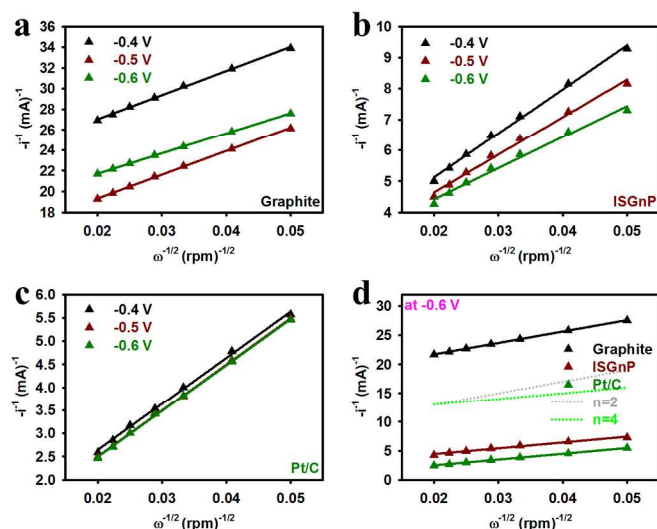


Fig. 5. Koutecky-Levich plots derived from RDE measurements at different electrode potentials: (a) Pristine graphite; (b) ISGnP; (c) Pt/C; (d) Comparison of the Koutecky-Levich plots at -0.6 V electrode potential. ISGnP and Pt/C are a four-electron transfer process, while the pristine graphite is close to a classical two-electron process.

Conclusion

We were able to synthesize edge-iodine/sulfonic acid-functionalized graphene nanoplatelets (ISGnP) *via* stepwise ball-milling of graphite with iodine initially and subsequently with sulfur trioxide. The structure of the resultant ISGnP was confirmed by various microscopic and spectroscopic analyses. Due to the polar functional groups, the dispersibility of ISGnP in various polar solvents is good enough for solution processing to form electrodes. Heteroatom doping enhances the polarity and oxygen-diffusion, and thus the ISGnP displayed superior electrocatalytic activity for ORR compared to commercial Pt/C. The thermodynamic control of ORR contributed to the enhanced oxygen adsorption and electron transfer, which were induced by edge-functional groups (iodine and sulfonic acid) on the graphitic framework. The kinetic contribution was related to oxygen diffusion by the polar nature of the edge functional groups as well. More importantly, ISGnP displayed better cycle stability compared with Pt/C. Considering scalable productivity, edge-selectivity and manufacturing simplicity, the ball-milling approach is considered to be an eco-friendly, low-cost, simple general method compared to existing GO/rGO and CVD approaches. Hence, ISGnP can be a strong potential alternative to expensive Pt/C electrocatalyst.

Acknowledgements

This work was supported by Mid-Career Researcher (MCR), BK21 Plus, Basic Research Laboratory (BRL) and Basic Science Research (BSR) programs through the National Research Foundation (NRF) of Korea, and the US Air Force Office of Scientific Research (AFOSR).

Notes and references

^a School of Energy and Chemical Engineering/Low-Dimensional Carbon Materials Center, Ulsan National Institute of Science and Technology (UNIST), 100 Banyeon, Ulsan 689-798, South Korea.

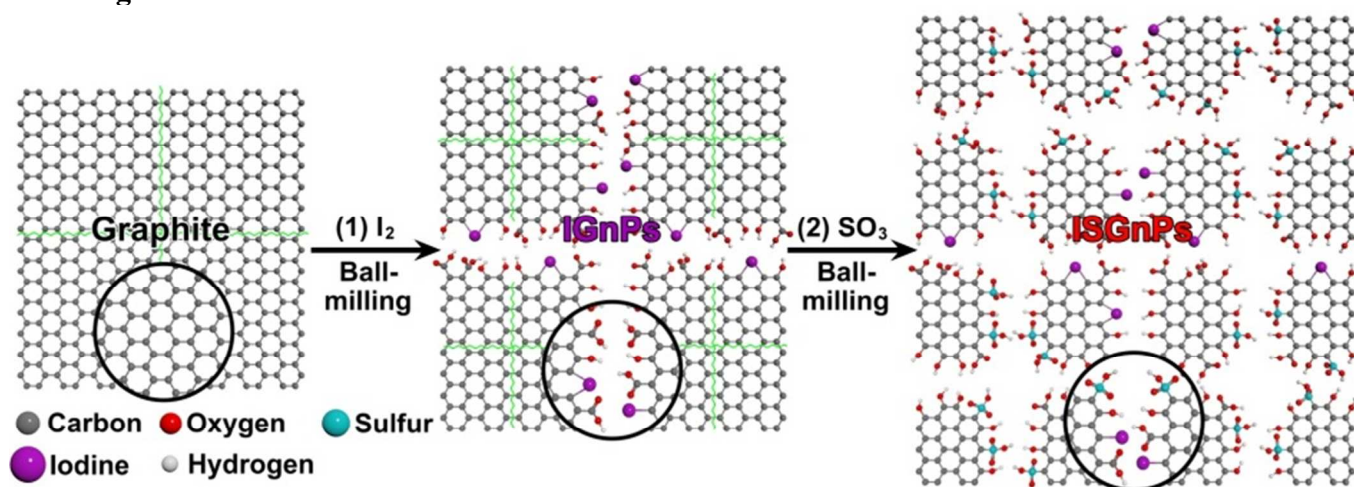
E-mail: jbbaek@unist.ac.kr

† Electronic Supplementary Information (ESI) available: [Experimental details of materials characterizations and electrochemical analyses]. See DOI: 10.1039/b000000x/

- 1 D. S. Yu, E. Nagelli and F. Du, L. Dai, *J. Phys. Chem. Lett.*, 2010, **1**, 2165.
- 2 Z.-L. Wang, D. Xu, J.-J. Xu, X.-B. Zhang, *Chem. Soc. Rev.*, 2014, DOI: 10.1039/C3CS60248F.
- 3 D. S. Su, J. Zhang, B. Frank, A. Thomas, X. Wang, J. Paraknowitsch and R. Schlögl, *ChemSusChem.*, 2010, **3**, 169.
- 4 L. Qu, Y. Liu, J.-B. Baek and L. Dai, *ACS Nano*, 2010, **4**, 1321.
- 5 S. Stankovich, D. A. Dikin, R. D. Piner, K. A. Kohlhaas, A. Kleinhammes, Y. Jia, Y. Wu, S. T. Nguyen and R. S. Ruoff, *Carbon*, 2007, **45**, 1558.
- 6 I.-Y. Jeon, H.-J. Choi, M. J. Ju, I. T. Choi, K. Lim, J. Ko, H. K. Kim, J. C. Kim, J. J. Lee, D. Shin, S.-M. Jung, J.-M. Seo, M.-J. Kim, N. Park, L. Dai and J.-B. Baek, *Sci. Rep.*, 2013, **3**, 2260.

- 7 Z. H. Sheng, H. L. Gao, W. J. Bao, F. B. Wang and X. H. Xia, *J. Mater. Chem.*, 2012, **22**, 390.
- 8 D. Long, W. Li, L. Ling, J. Miyawaki, I. Mochida and S.-H. Yoon, *Langmuir*, 2010, **26**, 16096.
- 9 Z. Yang, Z. Yao, G. F. Li, G. Fang, H. Nie, Z. Liu, X. Zhou, X. Chen and S. Huang, *ACS Nano*, 2012, **6**, 205.
- 10 H. L. Poh, P. Šimek, Z. Sofer and M. Pumera, *Chem. Eur. J.*, 2013, **19**, 2655.
- 11 I.-Y. Jeon, H.-J. Choi, M. Choi, J.-M. Seo, S.-M. Jung, M.-J. Kim, S. Zhang, L. Zhang, Z. Xia, L. Dai, N. Park and J.-B. Baek, *Sci. Rep.*, 2013, **3**, 1810.
- 12 W. S. Hummers and R. E. Offeman, *J. Am. Chem. Soc.*, 1958, **80**, 1339.
- 13 X. Fan, W. Peng, Y. Li, X. Li, S. Wang, G. Zhang and F. Zhang, *Adv. Mater.*, 2008, **20**, 4490.
- 14 H. A. Becerril, J. Mao, Z. Liu, R. M. Stoltenberg, Z. Bao and Y. Chen, *ACS Nano*, 2008, **2**, 463.
- 15 S. Park and R. S. Ruoff, *Nat. Nanotechnol.*, 2009, **4**, 217.
- 16 I.-Y. Jeon, Y.-R. Shin, G.-J. Sohn, H.-J. Choi, S.-Y. Bae, J. Mahmood, S.-M. Jung, J.-M. Seo, M.-J. Kim, D. W. Chang, L. Dai and J.-B. Baek, *Proc. Natl. Acad. Sci. U. S. A.*, 2012, **109**, 5588.
- 17 I.-Y. Jeon, H.-J. Choi, S.-M. Jung, J.-M. Seo, M.-J. Kim, L. Dai and J.-B. Baek, *J. Am. Chem. Soc.*, 2013, **135**, 1386.
- 18 I.-Y. Jeon, S. Zhang, L. Zhang, H.-J. Choi, J.-M. Seo, Z. Xia, L. Dai and J.-B. Baek, *Adv. Mater.*, 2013, **25**, 6138.
- 19 J.-M. Seo, I.-Y. Jeon and J.-B. Baek, *Chem. Sci.*, 2013, **4**, 4273.
- 20 M. Phaner-Goutorbe, A. Sartre and L. Porte, *Microsc. Microanal. Microstruct.*, 1994, **5**, 283.
- 21 H.-F. Wang, X.-Y. Deng, J. Wang, X.-F. Gao, G.-M. Xing, Z.-J. Shi, Z.-N. Gu, Y.-F. Liu and Y.-L. Zhao, *Acta Phys.-Chim. Sin.*, 2004, **20**, 673.
- 22 Z. Q. Li, C. J. Lu, Z. P. Xia, Y. Zhou and Z. Luo, *Carbon*, 2007, **45**, 1686.
- 23 P. G. de Gennes and *Rev. Mod. Phys.*, 1985, **57**, 827.
- 24 K. Gong, F. Du, Z. Xia, M. Durstock and L. Dai, *Science*, 2009, **323**, 760.
- 25 K. A. Mauritz and R. B. Moore, *Chem. Rev.*, 2004, **104**, 4535.

TOC Figure



Edge-iodine/sulfonic acid-functionalized graphene nanoplatelets (ISGnP) were prepared *via* two-step sequential ball-milling of graphite. The resultant ISGnP is highly dispersible in various polar solvents, allowing an easy fabrication of electrodes for ORR using solution processing. More importantly, the ORR performance of ISGnP in an alkaline medium is superior to commercial Pt/C in terms of electrocatalytic activity and cycle stability.